Journal of Physics: Conference Series

PAPER • OPEN ACCESS

Performance and midspan wake measurements on a H-Darrieus in controlled conditions

To cite this article: L. Battisti *et al* 2018 *J. Phys.: Conf. Ser.* **1037** 022041

IOP Conf. Series: Journal of Physics: Conf. Series **1037** (2018) 022041 doi:10.1088/1742-6596/1037/2/022041

Performance and midspan wake measurements on a H-Darrieus in controlled conditions

L. Battisti[1], **A. Brighenti**[1], **M. Raciti Castelli**[1]
G. Persico[2], **V. Dossena**[2]

[1] Department of Civil, Environmental and Mechanical Engineering, University of Trento, IT

[2] LFM - Laboratory of Fluid Machines, Energy Department, Politecnico di Milano, IT

E-mail: marco.raciticastelli@unitn.it

Abstract. Performance and wake measurements on a H-Darrieus vertical axis wind turbine are discussed on the basis of an extensive experimental campaign performed at the large scale, high speed wind tunnel of the Politecnico di Milano (IT). The paper proposes a combined mechanical and fluid-dynamic investigation by virtue of an advanced measurement system that allows to reconstruct both phase-resolved thrust and torque acting on the machine and the phase-resolved multi-dimensional velocity field in the wake. The aerodynamic torque is presented as a function of the azimuthal angle of revolution, while the velocity field in the wake is fully characterized by means of a point to point detailed measurement on the midspan plane, where the influence of both blade support struts and tip vortices is negligible.

Particular care is taken in the description of the experimental setup as well as in the presentation of the measurements. The here proposed achievements can be considered as a benchmark for the validation of several classes of computational tools.

Keywords: VAWT experimental data, wind tunnel testing, rotor wakes.

1. Introduction

In the last decade considerable interest was registered in vertical axis wind turbines (VAWTs), that indisputably exhibit a certain number of advantages over their horizontal axis counterparts, mainly in turbulent wind conditions that generally characterize the urban setting. Nonetheless, a widespread industrial implementation of such technology is still far from being achieved, due to several challenges posed by their intrinsic flow complexity (three-dimensional wake structures, double interaction between the blades and the streamtube during a revolution, highly unsteady blade loading, dynamic stall, etc.). As a consequence, the flow field past a VAWT is still far from being completely understood, calling for experimental investigations to convert an improved physical comprehension into newly developed aerodynamic models suitable to support the design phase. In particular, the prediction of extreme and fatigue loads are crucial for the proper structural design of the rotor; similarly, the accurate and realistic representation of the highly unsteady evolution of VAWT wakes remains a challenging task for aerodynamic prediction tools, especially for those conditions that trigger the onset of severe dynamic stall on the blade profiles.

By now, the most adopted simulation tool is the blade element momentum (BEM) model, originally proposed in the '70s in simple formulations (single disk - single streamtube [1] and,

later, single disc - multiple streamtubes [2]) and successively refined (double disk - multiple streamtubes [3]) also by resorting to several sub-models to account for the finite blade length, dynamic stall [4, 5], streamtube expansion [3], and flow curvature [6]. Also vortex methods (which compute the flow field from the blade circulation, as well as the trailing and shed vorticity) have been developed with the aim of providing a more realistic simulation of the wake unsteady behaviour [7, 8, 9, 10, 11, 12, 13]. The formulation of these latter methods introduces relevant flow features within the representation of turbine aerodynamics, both in terms of wake induction and flow unsteadiness, and have been recently found to provide realistic pictures of the wake flow as well as good predictions of the turbine performance [14]; they demand, anyway, a significant modeling effort supported by a systematic validation process. Finally, Computational Fluid Dynamic (CFD) is the most recent performance prediction model, generally based on the Reynolds Averaged Navier Stokes (RANS) equations [15, 16, 17, 18, 19] or on the Large-Eddy Simulation model [20, 21], that allow to compute the entire flow field surrounding a VAWT. The inherent capability of CFD of reproducing the flow physics makes this method less prone to the reliability issues that affect the other approaches. However, it still requires validation (especially in case flow separation occurs); moreover, the very high computational cost of CFD simulations, especially for VAWT [22], sets several limitations to its wide adoption, which is generally confined to research purposes.

The proper validation of both vortex models and CFD codes requires a detailed knowledge of the turbine wake downstream the rotor, possibly including the time-mean and time-resolved wake induction as well as the turbulence properties. Moreover, all numerical codes (BEM included) are capable of predicting the evolution of aerodynamic torque and thrust over a full rotation of the turbine, calling for phase-resolved data and thus allowing an in-depth validation. Nevertheless, a general lack of experimental data is recognized.

Following an experimental research program funded by the MIUR (Italian Ministry of Education, University and Research), part of the results obtained in a wind tunnel experimental campaign on a H-Darrieus rotor are here used to provide some evidence of the link between time-dependent torque (and thrust) measurements and wake characteristics, with the aim of supporting the interpretation of the rotor aerodynamics and of providing valuable experimental benchmark data for the validation of advanced numerical codes.

2. Experimental methodology

The hereby proposed experiments were performed in the large scale **wind tunnel** of the Politecnico di Milano, using the high speed section (4.00 m wide, 3.84 m high) in a free-jet configuration (obtained operating the rotor in a jet boundary confined environment). High flow quality was assured by a combination of honeycombs and anti-turbulence screens, leading to a freestream turbulence intensity lower than 1% at the test section.

The **tested rotor** is a straight-bladed Darrieus wind turbine with a swept area of 1.5 m^2, a solidity Nc/D of 0.25, and a blade section characterized by the classical NACA 0021 airfoil with a chord of 85 mm. Figure 1 provides a view of the test arrangement, showing both the open jet chamber and the instrumented rotor. The air flow velocity was limited to 9 m/s in the present experiment, and the rotor rotational velocity was kept constant to 400 rpm during the test by means of an inverter-controlled electrical machine; the blades rotate counter-clockwise. The resulting tip-speed ratio $\omega R/V_0$ was 2.4 and the chord Reynolds number was to 1.2 x 10^5, as reported in Table 1.

The quantification of the resulting free-jet blockage was conducted using established correlations available in literature [23, 24]. The resulting global blockage correction coefficient was close to 1.5% and was therefore considered negligible for the scope of the present work.

Rotor type	H-Darrieus
Blade number (N)	3
Height (H)	1.46 m
Diameter (D)	1.03 m
Chord (c)	0.085 m
Chord-to-radius ratio (2c/D)	0.17
Blade aspect ratio (H/c)	17.2
Blade profile	NACA0021
Rotor swept area (A)	1.5 m^2
Solidity (N c/D)	0.25
Rotor speed (Ω)	400 rpm
Blade Reynolds number (Re_c)	1.2 x 10^5
Wind speed (V_0)	9 m/s
Tip-speed ratio (TSR)	2.4
Air density (ρ)	1.208 kg/m^3

Figure 1. Pitcure of the wind tunnel open chamber with the rotor and the wake measurement system (on the right), and Table with rotor geometrical parameters and test operating condition.

The **measurement system**, briefly recalled in the present section, is extensively reported in [25]. Rotor angular velocity and position were provided by an absolute encoder, while the aerodynamic torque transmitted through the shaft was measured by means of a precision torquemeter mounted between elastic joints. The torque measurements were adjusted adding the tare torque to account for the friction in the system (2.3% of the peak torque). A synchronous motor/generator was installed on the power train and controlled using an inverter, thus assuring a constant rotational speed during the whole measurement campaign. To measure the flow in the wake, two single-sensor hot wires were traversed on the midspan section downstream of the rotor, thus providing the time-resolved stream-wise and cross-stream velocity components. The instantaneous velocity measurements were further processed to extract, by virtue of the triple decomposition, the phase-resolved (periodic) and turbulent velocity components. The 'intensity' of the periodic component was also calculated, defined as the root mean square of the periodic velocity fluctuation, to highlight synthetically the wake regions affected by the periodic blade motion (see [25] for an extended discussion on the post-processing technique applied in this study). Statistical tools were also applied to process the turbulent components and to determine, thanks to the angular sensitivity of the hot wire, the components of the Reynolds stress tensor related to the stream-wise and cross-stream turbulent velocity fluctuations (see [26]). Uncertainty in the wake velocity measurements resulted about 2% after calibration on a low-speed jet.

3. Results

In this section phased-resolved data of main rotor aerodynamic loads (torque and streamwise thrust) oscillation are presented during a rotation, as well as the velocity and turbulence properties in the wake developing downstream of the rotor. Experimental results are shown for TSR of 2.4, which is very close to the peak power coefficient condition ($C_{P,max}$=0.27). Such value, apparently low for a small VAWT, was nevertheless confirmed from further experimental investigation [27] and also from numerical works [15, 19] on the rotor considered in this study. In light of the extensive experimental and computational studies performed by the authors on this turbine, it is the authors' opinion that such a low value could be ascribed to the combined effects of high solidity and considerable spoke dimensions.

The basic working principle of lift-driven VAWT rotor is as follows. As the vertically straight blades of the turbine turn about the central shaft, both the magnitude and the direction of the effective velocity perceived by the blades change in a cyclic manner. It followed that blade

aerodynamic loads change cyclically during a revolution.
Figure 2 and 3 respectively show the torque and streamwise thrust fluctuation as a function of the azimuthal blade position. The azimuthal angle θ is set to be zero when the blade is parallel and upwind respect to the incoming flow V_0, and it increases in counter-clockwise direction. As expected for a rotor three-blade architecture, the three per revolution (3P) oscillation dominates, and a periodicity of 120° is clearly registered.

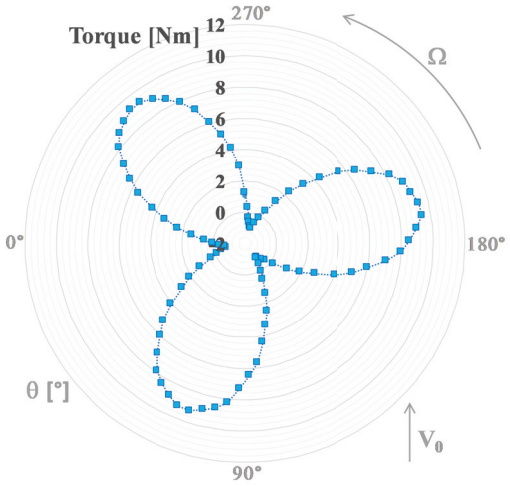

Figure 2. Phased torque fluctuation as a function of the azimuthal blade position θ (TSR = 2.4).

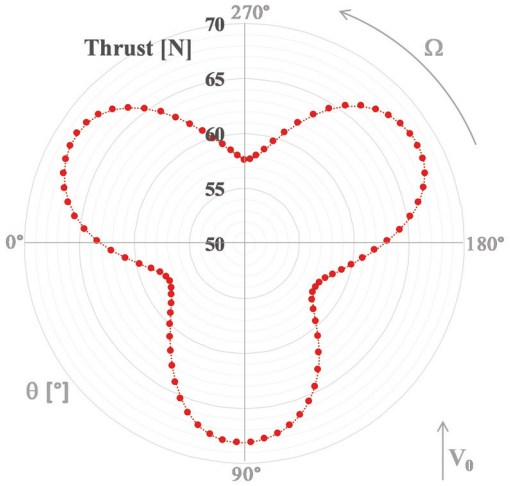

Figure 3. Phased streamwise thrust fluctuation as a function of the azimuthal blade position θ (TSR = 2.4).

The *torque data* (Figure 2) show a first peak at a relative rotor position θ of 50°, in according to the Sandia test results [28], ranging approximately between 9.5 to -1.0 Nm. The mean value is 4.24 Nm ± 0.13 Nm, where the last figure expresses the uncertainty on torque measurements [29]. Also the *streamwise thrust data* (Figure 3) show an almost cosine curve, showing the first peak at θ of 90°, shifted respect to the torque peak. The mean value is 63.03 N ± 0.85 N, and thrust data ranges approximately between 68.2 to 57.6 Nm.
In general for VAWTs operating in actual open-field environments, the aerodynamic loads can vary strongly during a rotation cycle resulting in strong time-dependent loads. During this test, the rotor undergoes relevant aerodynamic torque fluctuations and more moderate streamwise thrust oscillations, in spite of the fact that the incoming wind speed is unchanging. It is, therefore, interesting to investigate the development and the unsteady evolution of the turbine wake downstream of the rotor.

The wake downstream of the rotor was investigated by means of time-resolved hot-wire measurements on a plane surface placed at midspan. By virtue of the extension of the probe traversing system, the streamwise travesing extends from X/R = 0.8 to X/R = 2.4 on the lateral sides and from X/R = 1.35 to X/R = 2.4 in the central section (a minimum safety distance of 110 mm was imposed between the probes and the rotor blades). In this way, the area covered by the measurement surface allows to analyze experimentally the near-wake development both in the central region (where dynamic-stall vortices are deteched, see [10, 13]) as well on the lateral sides of the rotor, where the wake sides establish.

Figures 4 and 5 report the distribution of the time-mean velocity components as measured on the resulting midspan surface. Figure 6 reports the field of the corresponding time-mean flow angle, constructed combining the time-mean stream-wise and cross-wise velocity components;

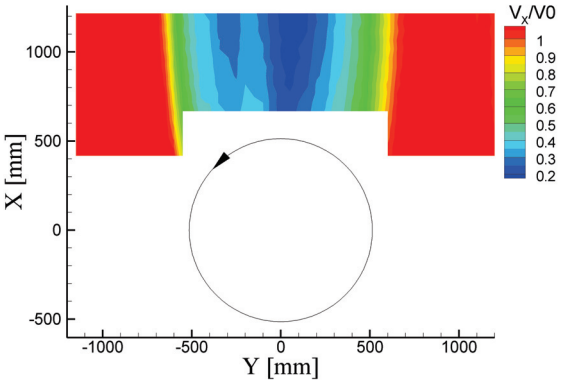

Figure 4. Distribution of time-mean velocity component in streamwise direction on the midspan surface downstream of the rotor, made non dimensional with the upstream free-stream velocity, TSR = 2.4.

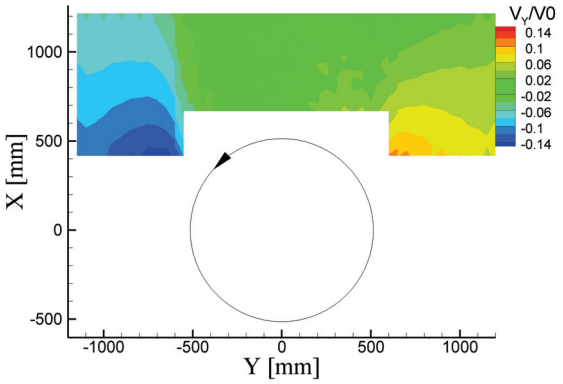

Figure 5. Distribution of time-mean velocity component in cross-stream direction on the midspan surface downstream of the rotor, made non dimensional with the upstream free-stream velocity, TSR = 2.4.

cross-stream components and flow angles are taken positive for flows oriented towards the right. The wake picture emerging from these maps is consistent with the general features of VAWT wakes documented in previous experimental studies [10, 30, 31, 32, 33, 25]. However, thanks to the extension of the measurement area, the level of detail provided by the instrumentation, and the peculiar data-processing applied to the unsteady velocity measurements, relevant novel features appear.

The distribution of velocity components show that the typical asymmetry of the VAWT wake is more significant close to the rotor and a more symmetric shape tends to be recovered at about 1 D from the shaft. Relevant cross-stream components appear on the wake sides, mostly connected to the enlargement of the streamtube passing through the rotor. The (negative) cross-stream components are slightly more pronounced on the left side of the wake (i.e., the one resulting from the 'windward' side of the blade rotation). This is consistent with the slight shift of the wake towards the left, which corresponds to windward side of the turbine (where the blades retreat), which is consistent with the flow angle changes in transversal direction; a lower velocity deficit is also found in this region. It is interesting to note that, close to the rotor blades, non-negligible flow angle components arise also in the right side of the wake (i.e., the one resulting from the 'leeward' side of the blade rotation).

Figure 7 reports the intensity of periodic unsteadiness of the velocity magnitude, as measured on the midspan measurement surface. Such quantity highlights the deterministic fluctuations locked to the blade motion, and shows that both the sides of the wake are affected by periodic oscillations. The oscillations affect a wider area on the leeward side of the wake; this is the impact on the wake of the higher fluctuations of Reynolds number and angle of attack that the blades experience in this phase of the rotation. In the core of the wake, the deterministic unsteadiness exhibits a nearly symmetric distribution and rapidly decays from relatively high values to almost null at about one turbine diameter far from the shaft. The significant periodic oscillations measured close to the rotor over the entire section of the wake are fully consistent with the periodic oscillations of torque and thrust experienced by the turbine, and shows that VAWT aerodynamics are highly unsteady not just at low TSR but also close to peak efficiency; this was also observed in the flow prediction obtained with recent CFD simulations performed in the midspan section of this rotor [19], which suggest the onset of highly unsteady flow close to the rotor for TSR = 2.4 (even though no relevant dynamic stall was found to occur in the

windward and upwind phases of the rotation in this TSR condition).

In order to investigate the turbulence properties of the wake, the unresolved unsteadiness of the velocity signals were processed to extract the components of the Reynolds stress tensor. In particular, the diagonal Reynolds stresses representing the streamwise and cross-stream turbulence components were processed to obtain the corresponding turbulence intensities, and are reported in Figures 8 and 9. Higher turbulence appear on both the wake sides, with clearly higher values on the leeward side of the wake. A further peak of streamwise turbulence intensity is visible in the center of the wake, clearly connected to the wake of the shaft, which also induces the highest velocity deficit in the wake. It is interesting to note that, differently from what found for the deterministic components, the decay of turbulence is much slower and the asymmetry in the wake remains fully visible also at the maximum distance from the rotor.

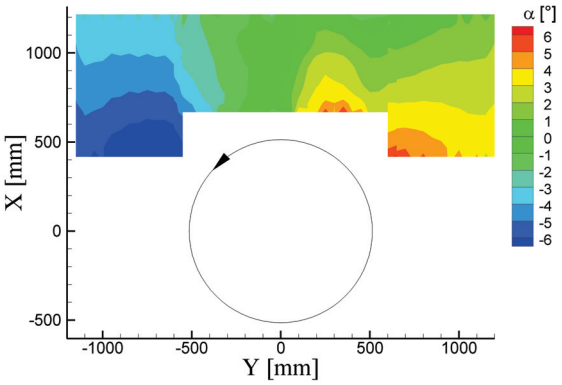

Figure 6. Distribution of the flow angle on the midspan surface downstream of the rotor, evaluated between the stream-wise and cross-stream velocity components, TSR = 2.4.

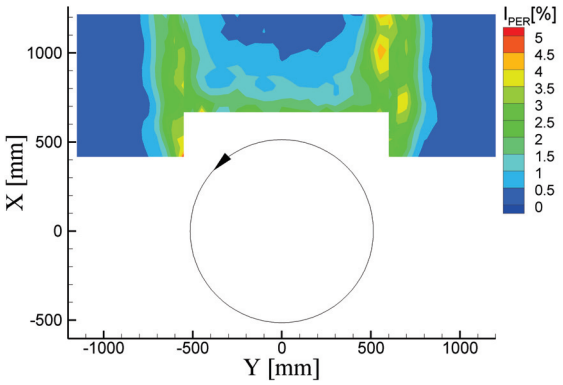

Figure 7. Distribution of the intensity of periodic unsteadiness of the velocity magnitude on the midspan surface downstream of the rotor, made non dimensional with the upstream free-stream velocity, TSR = 2.4.

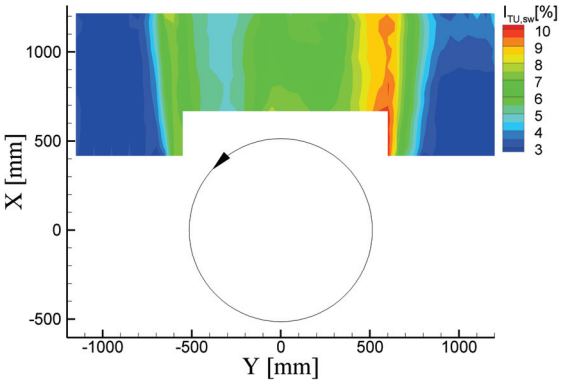

Figure 8. Distribution of streamwise turbulence intensity on the midspan surface downstream of the rotor, referred to the upstream free-stream velocity, TSR = 2.4.

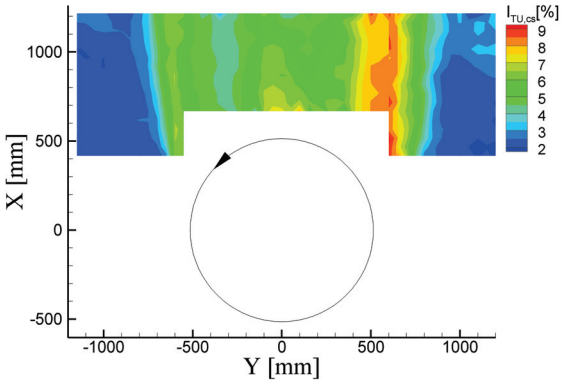

Figure 9. Distribution of cross-stream turbulence intensity on the midspan surface downstream of the rotor, referred to the upstream free-stream velocity, TSR = 2.4.

4. Conclusion

This paper has presented a novel set of measurements on a H-shaped VAWT whose time-averaged performance was studied in the past. In particular, the phase-resolved torque and stream-wise thrust measured by means of dedicated on-shaft instrumentation have been reported for an operating condition close to the peak efficiency. High unsteady fluctuations have been recorded, especially on the torque that oscillates by $\pm 100\%$ with respect to the time-mean value. More moderate oscillations have been found for the stream-wise thrust, that amount to less than $\pm 10\%$ with respect to the time-mean value.

The unsteady aerodynamics of the rotor has an evident consequence on the unsteady wake structure. Detailed velocity and turbulence measurements on a midspan surface downstream of the rotor allow to appreciate the near-wake evolution in terms of velocity components, periodic unsteadiness and turbulence. The wake evolves significantly near to the rotor blades, resulting highly asymmetric and highly unsteady close to the rotor. Within 1D of streamwise distance from the shaft most of the deterministic unsteadiness decays and the wake become almost symmetric. Conversely, the turbulence in the wake undergoes a much lower decay rate and the near-wake features are retained for the whole area covered by the measurement surface.

The observed features, as well as the level of detail provided by the torque and wake measurements, add a set of valuable data for the comprehension of VAWT aerodynamics and for the validation of advanced numerical codes.

List of symbols

Latin

A	rotor swept area [m^2]
B	rotor blade number [-]
c	airfoil chord length [m]
H	rotor height [m]
I_{TU}	turbulence intensity [-]
Re_c	chord Reynolds number = ω R c/ ν [-]
t	airfoil thickness [m]
TSR	tip-speed ratio = ω R / V_0 [-]
V_0	freestream wind speed [m/s]
V_X	local streamwise wind speed [m/s]
V_Y	local cross-stream wind speed [m/s]
I_{PER}	intensity of periodic unsteadiness [%]
$I_{TU,SW}$	streamwise turbulence intensity [%]
$I_{TU,CS}$	cross-stream turbulence intensity [%]

Greek

θ	azimuthal blade position [°]
ν	freestream kinematic viscosity [m^2/s]
ρ	freestream density [kg/m^3]
σ	rotor solidity = B L c / A [-]
Ω	rotor angular velocity [rpm]
ω	rotor angular velocity [s−1]
α	flow angle between streamwise and cross-stream components [deg]

Acronyms

BEM	Blade Element-Momentum
HAWT	Horizontal Axis Wind Turbine
VAWT	Vertical Axis Wind Turbine

References

[1] Templin R.S. (1974) *Aerodynamic Performance Theory for the NRC Vertical-Axis Wind Turbine*. National research Council of Canada, Ottawa, LTR-160, 1974.

[2] Strickland J.H. (1975) *The Darrieus Turbine: A Performance Prediction Model Using Multiple Streamtubes*. Sandia National Laboratories, Albuquerque, New Mexico, SAND75-0460, 1975.

[3] Paraschivoiu I. (2002) *Wind Turbine Design - With Emphasis on Darrieus Concept*. Polytechnic International Press: Montral, Canada, 2002.
[4] Masse B. (1981) *Description of two Programs for Calculating Performance and Aerodynamic Loads of a Vertical Axis Wind Turbine*. Institut de recherche de l'Hydro, Québec, Canada, 1981.
[5] Berg D.E. (1983) *An Improved Double-Multiple Streamtube Model for the Darrieus-Type Vertical Axis Wind Turbine*. In Proceedings of the 6th Biennal Wind Energy Conference and Workshop, Minneapolis, MN, USA, 13 June 1983, pp. 231-233.
[6] Migliore P.G., Wolfe W.P., Fanucci J.B. (1980) *Flow curvature effects on Darrieus turbine blade aerodynamics*. Journal of Energy, Vol 4, pp. 49-55.
[7] Larsen H.C. (1975) *Summary of a vortex theory for the cyclogiro. Proceedings of the second US national conferences on wind engineering research*, Colorado State University, 1975, p. V8-13.
[8] Strickland J.H., Webster B.T., Nguyen T.(1979) *A Vortex model of the Darrieus turbine: an analytical and experimental study* Journal of Fluids Engineering, Vol 101.
[9] Cardona J.L. (1984) *Flow curvature and dynamic stall simulated with an aerodynamic freevortex model for VAWT*, Wind Engineering, 1984, Vol. 8, pp. 135-143.
[10] Ferreira J.S. (2009) *The Near Wake of the VAWT: 2D and 3D Views of the VAWT Aerodynamics*, Ph.D. Thesis, Delft University of Technology, the Netherlands, 2009.
[11] Scheurich F., Fletcher T.M., Brown R.E. (2011) *Simulating the Aerodynamic Performance and Wake Dynamics of a Vertical-Axis Wind Turbine*, Wind Energy, Vol 14(2), pp. 159-177.
[12] Scheurich F., Brown R.E. (2013) *Modelling the Aerodynamics of Vertical-Axis Wind Turbines in Unsteady Wind Conditions*, Wind Energy, Vol. 16(2), pp. 91-107.
[13] Chetelain P., Duponcheel M., Caprace D.G., Marichel Y., Winckelmans G. (2016) *Vortex Particle-Mesh simulations of Vertical Axis Wind Turbine flows: from the blade aerodynamics to the very far wake*, Journal of Physics: Conference Series, Vol. 753, paper number 032007.
[14] Saverin J., Persico G., Marten D., Holst D., Pechlivanoglou G., Paschereit C.O., Dossena, V. (2017) *Comparison of Experimental and Numerically Predicted Three-Dimensional Wake Behaviour of a Vertical Axis Wind Turbine*, Proc. ASME Turbo Expo 2017, June 26-30, 2017, Charlotte, NC USA
[15] Trivellato F., Raciti Castelli M. (2014) *On the Courant-Friedrichs-Lewy criterion of rotating grids in 2D vertical-axis wind turbine analysis*, Renewable Energy, Vol. 62, pp. 53-62.
[16] Trivellato F., Raciti Castelli M. (2015) *Appraisal of Strouhal number in wind turbine engineering*, Renewable and Sustainable Energy Review, Vol. 49, pp. 795-804.
[17] Lam H.F., Peng H.Y. (2016) *Study of wake characteristics of a vertical axis wind turbine by two and three-dimensional computational fluid dynamics simulations*, Renewable Energy, Vol. 90, pp. 386-398.
[18] Raciti Castelli M., Masi M., Battisti L., Benini E., Brighenti A., Dossena V., Persico G. (2016) *Reliability of numerical wind tunnels for VAWT simulation* in Journal of Physics: Conference Series, 753, paper number 082025.
[19] Bianchini A., Balduzzi A., Ferrara G., Ferrari L., Persico G., Dossena V., Battisti L. (2018) *Detailed analysis of the wake structure of a straight-blade H-Darrieus wind turbine by means of wind tunnel experiments and CFD simulations*, Journal of Engineering for Gas Turbines and Power, Vol. 140, paper number 032604.
[20] Shamsoddin S., Porté-Agel F. (2014) Large Eddy Simulation of Vertical Axis Wind Turbine Wakes, Energies, Vol. 7, pp. 890-912
[21] Abkar M., Dabiri J.O. (2017) Self-similarity and ow characteristics of vertical-axis wind turbine wakes: an LES study, Journal of Turbulence, Vol. 18, pp. 373-389.
[22] Balduzzi F., Drofelnik J., Bianchini A., Ferrara G., Ferrari L., Campobasso M.S. (2017) Darrieus wind turbine blade unsteady aerodynamics: a three-dimensional Navier-Stokes CFD assessment, Energy, Vol. 128, pp. 550-563
[23] Glauert H. (1947) *The Elements of Aerofoil and Airscrew Theory*. Cambridge University, Cambridge, GB, 2nd Ed., 1947.
[24] Mikkelsen R., Sørensen J.N. (2002) *Modelling of Wind Tunnel Blockage* in Proceedings of the Global Windpower Conference and Exhibition, 2002.
[25] Persico G., Dossena V., Paradiso B., Battisti L., Brighenti A., Benini E. (2017) *Time-Resolved Experimental Characterization of the Wakes Shed by H-shaped and Troposkien Vertical Axis Wind Turbines*, Journal of Energy Resources Technology, Vol. 139, paper number 031203.
[26] Perdichizzi, A., Ubaldi, M., Zunino, P. (1990) *A hot wire measuring technique for mean velcity and Reynolds stress components in compressible flow*, Proc.10th Symposium on Measuring Techniques for Transonic and Supersonic Flows in Cascades and Turbomachinery, 1990.
[27] Battisti L., Persico G., Dossena V., Paradiso B., Raciti Castelli M., Brighenti A., Benini E. (2018) *Experimental benchmark data for H-shaped and troposkien VAWT architectures*, Renewable Energy, Vol. 125, pp. 425-444.

[28] Akins R.E., Berg D.E., Tait Cyrus W. (1980) *Measurements and Calculations of Aerodynamic Torques for a VAWT*, Technical Report SAND86-2164, Sandia National Laboratories, October 1980
[29] ISO ENV 13005 (1999) *Guide to the Expression of Uncertainty in Measurement*
[30] Tescione G., Ragni D., He C., Ferreira C.J., van Bussel J.W. (2014) *Near wake flow analysis of a vertical axis wind turbine by stereoscopic particle image velocimetry.* Renewable Energy, Vol. 70, pp 47-61.
[31] Dossena V., Persico G., Paradiso B., Battisti L., Dell'Anna S., Benini E., Brighenti A. (2015) An experimental study of the aerodynamics and performance of a Vertical Axis Wind Turbine in confined and unconfined environment, Journal of Energy Resources Technology, Vol. 137, paper number 051207.
[32] Peng H.Y., Lam H.F., Lee C.F. (2016) *Investigation into the wake aerodynamics of a five-straight bladed vertical axis wind turbine by wind tunnel tests*, Journal of Wind Engineering and Industrial Aerodynamics, Vol. 155, pp. 23-35.
[33] Rolin V., Porté-Agel F. (2017). *Experimental investigation of vertical-axis wind-turbine wakes in boundary layer flow.* Renewable Energy, Vol. 118, pp. 1-13.